

# Measurement of the hydraulic properties of chalk using centrifuge permeameter; the study of chalk hydraulic properties under accelerated gravitational force



Peshawa Al-Jaf\*, Martin Smith and Friederike Gunzel

Cockcroft Building, University of Brighton, Lewes Road, Brighton BN2 4GJ, UK

PA, 0000-0002-4853-6758

\* Correspondence: [peshawa79@hotmail.com](mailto:peshawa79@hotmail.com)

**Abstract:** In this study, a geotechnical centrifuge has been used to study the unsaturated hydraulic properties of rock samples from the chalk aquifer, SE England. This method allows rapid measurement of hydraulic properties in a controlled environment, in contrast to previous studies on the chalk unsaturated zone, which required either an extended period (years) of data monitoring in the field or extended experimental periods (weeks) in the laboratory. Three types of specially built sensors were used to monitor water flow through chalk samples: a water pressure transducer to measure matric potential, frequency domain reflectometry probes to measure the volumetric water content and pressure transducers to measure the volume of water passing through the sample. Chalk samples were tested during wetting and draining processes to understand any hysteresis occurring during periodic recharge of the aquifer. Before undertaking physical tests of chalk samples in the centrifuge, a theoretical model of chalk hydraulic behaviour under centrifugal force was developed. This model was used to define and justify the instrumentation plan of the physical model and predict the shape of the soil moisture characteristic (SMC) curve and unsaturated hydraulic conductivity ( $K_u$ ) function. The results were then evaluated and compared with the experimental results. These results show that chalk samples can be successfully tested under centrifuge conditions and hydraulic properties can be measured, including soil moisture characteristic curves and hydraulic conductivity.

**Supplementary material:** Calculation spread sheets are available at <https://doi.org/10.17033/DATA.00000283>

**Received** 2 November 2021; **revised** 29 January 2022; **accepted** 4 April 2022

The Chalk Group of NW Europe is a major aquifer unit extending from Denmark to the UK and France, comprising micritic limestone composed dominantly of coccoliths (rock type chalk) with interbedded marl and flint layers (Downing *et al.* 1993). Chalk as a rock type offers a number of issues for aquifer characterization because of its dual porosity nature (Price *et al.* 1993), and the small pore size resulting in very low matric potentials and a very thick unsaturated zone (Price *et al.* 1976; Rutter *et al.* 2012). Matric potential is defined in the majority of the soil and groundwater literature as the pore fluid pressure head in unsaturated media (Or *et al.* 2005; Kirkham 2014; Lal 2017). Understanding of unsaturated zone flow is critically important for determination of aquifer recharge, contaminant transport and engineering implications of aquifer hydrology (e.g. Haria *et al.* 2003). Flow of water through intergranular pore space in the chalk unsaturated zone can be described using three related variables: matric potential ( $\psi$ ), volumetric water content ( $\theta$ ) and unsaturated hydraulic conductivity (Price *et al.* 1993) ( $K_u$ ) via the Richard's equation ((Richards 1931; Hiscock and Bense 2014). From the first two variables ( $\psi$ ,  $\theta$ ), it is possible to draw a soil moisture characteristic (SMC) curve. The curve describes the way in which water infiltrates or drains from the unsaturated zone at a certain volumetric water content ( $\theta$ ) and a given matric potential ( $\psi$ ), allowing definition of the unsaturated zone hydraulic gradient. The unsaturated hydraulic conductivity ( $K_u$ ) represents the proportionality between the flow rate and the hydraulic gradient, and is relevant only for the condition in which the water phase in the soil or rock is continuous (Zornberg and McCartney 2010).

Since the 1980s several studies have been carried out to study chalk unsaturated hydraulic properties based on theoretical calculations (indirect methods) or physical measurements (direct

methods). In both methods, field data are necessary, which requires borehole logging, plus several years of monitoring. Ireson (2008), Gallagher *et al.* (2012) and Rutter *et al.* (2012) studied the chalk unsaturated zone using specially built tensiometers, which were used to monitor change of the matric potential ( $\psi$ ) throughout the chalk unsaturated zone. Other studies, for example, those of Wellings (1984), Gardner *et al.* (1990), Haria *et al.* (2003) and Mathias *et al.* (2005), focused on the development of integral physical recharge models to reproduce long-term field observations. With the improvement in technology and the development of advanced sensors and instruments (miniature water pressure transducers and frequency domain reflectometry) it is now possible to measure these hydraulic properties within a very short period (hours to days) under a controlled environment. These new tools record data in a direct, fast and reliable way, allowing the accurate determination of SMCs and unsaturated hydraulic conductivity ( $K_u$ ) for application in computational models and understanding of unsaturated zone processes. The use of rapid, controlled, mesoscale measurement and modelling has the potential to provide key quantitative data on rock mass properties that complement data from field-scale measurements, which take into account macro-scale variation and hydraulic conditions that cannot be replicated in the laboratory (Hiscock and Bense 2014).

This work focuses on laboratory measurement of water flow through unsaturated chalk samples using a geotechnical centrifuge, which addresses a shortcoming of previous approaches in allowing rapid measurement of the hydraulic properties of chalk. This method has been used previously for rapid measurement of hydraulic properties of unsaturated soil. This was the motivation for the development of the steady-state centrifuge method by Nimmo *et al.* (1987) and unsaturated flow apparatus by Conca and

Wright (1992). Both studies determined hydraulic conductivity under steady-state conditions. However, these studies used a high-speed medical ultracentrifuge, which did not include a data acquisition system to allow direct and simultaneous measurements during in-flight conditions, which, consequently, did not permit the simultaneous measurement of the matric potential ( $\psi$ ) and volumetric water content ( $\theta$ ). This may have influenced their results. Also, both studies used a simplified equation in which the matric potential gradient was neglected. Hydraulic conductivity of unsaturated porous media is a function of gravimetric water content; this was measured by stopping the centrifuge periodically and measuring weight change in the sample until observation of a steady-state condition. In contrast, the results measured in the current study were obtained in-flight within the centrifuge, allowing direct and simultaneous measurement of matric potential ( $\psi$ ) and volumetric water content ( $\theta$ ). Therefore, the full form of Darcy's law under centrifugal acceleration could be applied (equation (5)), rather than the simplified form (equation (1)):

$$q = -K_{\psi} \left( \frac{d\psi}{dr} - \rho_w \omega^2 r \right) \quad (1)$$

where  $q$  is the Darcy flux ( $L T^{-1}$ ),  $\psi$  is the matric potential ( $M L^{-1} T^{-2}$ ),  $\rho_w$  is the density of water ( $M L^{-3}$ ),  $K_{\psi}$  is the hydraulic conductivity in the matric potential function ( $L T^{-1}$ ),  $\omega^2$  is the angular velocity ( $rad T^{-1}$ ) and  $r$  is the rotational axis ( $L$ ).

A geotechnical centrifuge was used in this study to produce a high acceleration environment (Fig. 1). The centrifuge can be used to subject a soil or rock specimen to high artificial gravity, allowing small-scale models tested over a short time to be representative of much larger real-life structures over a much longer period. Geotechnical centrifuge models have been widely used to simulate soil–structure interactions (White 2020), and in a range of rock mechanics applications including slope and tunnel stability (e.g. Feng and Yin 2014), and in hydrological investigations including non-aqueous phase liquid flow in aquifers (e.g. Levy *et al.* 2002). This high artificial gravity is produced by the centrifugal acceleration, which depends on the rotation speed and the radius of the beam around the rotational axis. We are not aware of any previous studies that have investigated chalk hydraulic behaviour under high acceleration; thus, a theoretical background is needed to understand its behaviour under such high acceleration before a real test is undertaken. Several approaches can be used to interpret the results from the centrifuge, including transient infiltration analysis, inverse analysis and steady-state infiltration analysis. The last was adopted by Moore (1939). In this study, the steady-state method is used to analyse the centrifuge results, which uses the data after

reaching equilibrium conditions for a known flow condition in the chalk sample.

### Method used in the study

Before conducting the centrifuge permeameter tests on chalk samples, a theoretical study of chalk under centrifuge conditions was conducted, based on the analytical solution to Richards' equation developed by Avanzi *et al.* (2004). Richards' equation describes flow in unsaturated medium at a steady-state condition (Richards 1931). The theoretical study used an exponential model to represent the hydraulic conductivity as a function of matric potential ( $\psi$ ) under steady-state flow. The theoretical calculations were used to determine the water flow and sensor locations in the sample. Details of the water flow and the location of the sensors are given in the Theoretical constraints section.

Samples of the Seaford and Lewes Nodular Chalk Formations were collected from Shoreham Quarry, West Sussex [520892, 109004], and cut to  $300 \times 180 \times 120$  mm size for use in the centrifuge permeameter. Both samples were selected to avoid visible marl seams, flint, macroscale fractures and karstic dissolution features. The Lewes Nodular Chalk sample consisted of hard, white, homogeneous chalk with no visible nodules. The Seaford Chalk sample consisted of firm, white, homogeneous chalk. The porosity varied from 36% in the Seaford Chalk to 33% in the Lewes Nodular Chalk Formation. The samples were glued to Plexiglas with silicone epoxy on the lateral sides to prevent lateral flow between the chalk sample and the sides of the sample container. The top and bottom parts of the chalk remained open to allow water to recharge on the upper surface and discharge from the lower face (Fig. 2). Water was added to the top of the samples using a Jasco 980U HPLC pump. Three water pressure transducers (wpt), and one frequency domain reflectometer (FDR) were attached to the chalk block to monitor changes in matric potential ( $\psi$ ) and volumetric water content ( $\theta$ ) respectively under centrifugal acceleration. The wpt sensor (Measurement Specialties, EPB-PW Miniature Pressure Transducer) has a rugged construction of titanium, and is not affected by external clamping force during use, particularly in centrifuge conditions. It has a miniature design of  $6.3 \times 11.4$  mm. It connects to the chalk sample through a 40 mm deep and 6.5 mm radius hole drilled in the lateral side of the chalk sample. A screw with a rubber O-ring and a spring is used to fix and stabilize the wpt sensor and prevent leaking. The FDR is a Decagon GS3, developed by Decagon Devices, Pullman, USA. The GS3 has a slim shape with dimensions 60, 20 and 70 mm, and the waveguides are three stainless steel prongs 55 mm long and 5 mm in diameter. Because

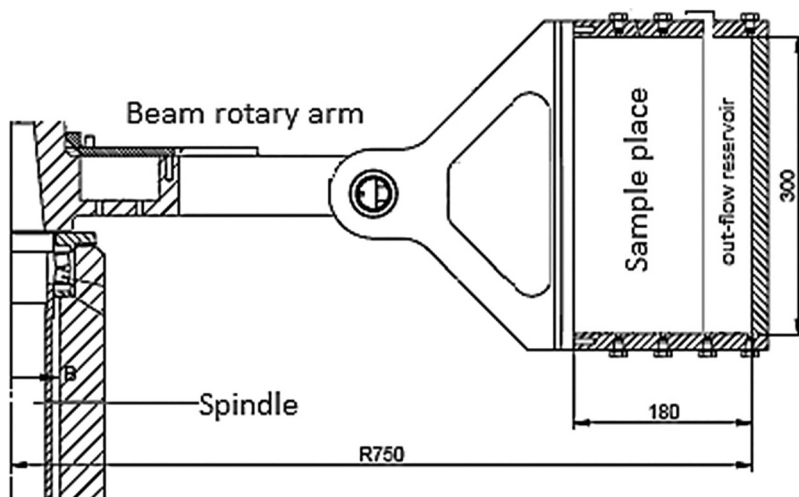


Fig. 1. The Broadbent centrifuge set-up showing the rotary beam and the sample cradle system used in this study.

## Hydraulic properties of chalk



**Fig. 2.** The chalk samples glued to Plexiglas on the lateral sides (a), and connection of the water pressure transducer (wpt) to the side of the chalk sample (b).

of its slim shape and stainless steel needles it is well suited for centrifuge modelling. It is connected to the chalk sample through three drilled holes (56 mm depth and 5.5 mm diameter) in the lateral side of the chalk sample (Fig. 3). Lateral flow is prevented by the use of a plastic O-ring connected to the prongs and a stabilizer. Also, a pressure transducer (pt) was used in the outflow reservoir to determine the volume of water that drained from the sample with time, and hence to determine the discharge rate in the reservoir below the sample. This pt is manufactured by Druck (model PDCR-81) and has dimensions of  $5.7 \times 9.5$  mm. The pt sensor measures the pressure of water added to the reservoir and the pressure was converted to the volume of water in the reservoir

by a calibrated equation. Finally, the results obtained from laboratory tests were compared with the theoretical results.

The high artificial gravity in a centrifuge is produced by the centrifugal acceleration resulting from high-speed rotation, which depends on the rotation speed and radius of the beam (rotational axis) according to equation (2):

$$g_r = \frac{\omega^2 r}{895} \quad (2)$$

where  $g_r$  is centrifugal acceleration ( $\text{m s}^{-2}$ ) (in this study we refer to the factor  $N_r$ , where  $N_r = g_r/g$  (multiple of the Earth's gravitational acceleration)),  $\omega$  is rotational speed ( $\text{rev min}^{-1}$ ),  $r$  is the radius from

## The Cradle

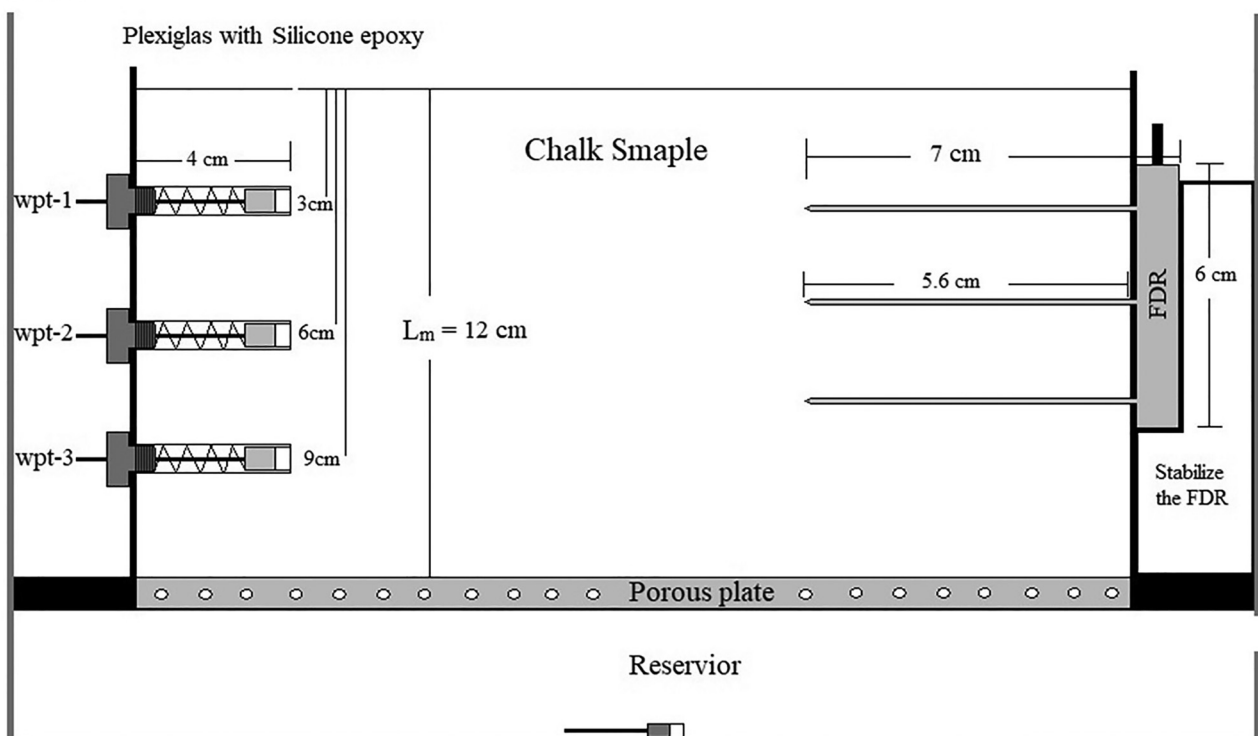


**Fig. 3.** Schematic diagram of the chalk sample inside the centrifuge: FDR, frequency domain reflectometer; wpt, water pressure transducers; pt, pressure transducer.

the axis of rotation (metres) and 895 is the conversion factor from  $\text{rev min}^{-1}$  to angular velocity ( $\text{rad s}^{-1}$ ).

A Broadbent geotechnical centrifuge (Geotechnical Beam Centrifuge GT6/0.75, 6 G-Toneee) was used in this study. The maximum rotation speed is  $638 \text{ rev min}^{-1}$  of the 750 mm beam, which is equivalent to 300g acceleration.

Two types of tests were undertaken: wetting and draining tests. The wetting tests were done by adding a known volume of water to an oven dry chalk sample and monitoring the gradual filling of the chalk matrix and fractures with water. Prior to each test the chalk sample was dried for 24 h at  $75^\circ\text{C}$ ; this temperature was used to avoid cracking of the chalk sample in the oven. Moreover, the duration and temperature are enough to dry the chalk sample to reach air entry pressure. The wetting test was carried out on eight samples and repeated on individual samples to check for reproducibility. The draining tests were carried out using chalk samples that had been saturated under vacuum for 48 h before the test. These were then allowed to drain under centrifuge force. The draining test was carried out for both intact and fractured chalk samples. In both test types, the matric potential ( $\psi$ ), volumetric water content ( $\theta$ ) and volume of water drained from the sample were monitored. Data were continuously measured during in-flight conditions, allowing direct determination of the flow processes in the chalk unsaturated zone. The matric potential ( $\psi$ ) was recorded at three levels with wpt sensors and the volumetric water content ( $\theta$ ) was measured with one FDR sensor. The main criteria in ending each test were that air entry pressure should be reached and at that point flow is restricted and no more water is drained to the reservoir. However, in test T6, the time of the test exceeded that limit to reach a minimum matric potential recorded under centrifuge conditions.

## Results

### Theoretical constraints

Early centrifuge technique studies (e.g. Briggs and McLane 1910; Gardner 1937) did not include steady-state flow through the sample. An initially saturated sample ( $\psi_0 = 0$  at mid-height of the sample ( $z_m$ )) was drained under centrifuge force, and the sample was said to be at equilibrium when the outflow stopped. In this case, the equilibrium  $\psi$  profile in the sample was determined from equation (3):

$$\psi(z_m) = \frac{\rho_w \omega^2}{2} [2r_0 z_m - z_m^2] + \psi(0). \quad (3)$$

Avanzi *et al.* (2004) developed an equation of the  $\psi$  profile during steady-state flow as follows:

$$\psi(z_m) = -\frac{1}{\alpha} \ln \left( \exp \left\{ \ln \left[ \frac{v_m}{(N_r K_s)} \right] + e^{-\alpha \psi_0} \right\} - \alpha \omega^2 \rho_w z_m \left[ r_0 - \left( \frac{z_m}{2} \right) \right] - \frac{v_m}{N_r K_s} \right) \quad (4)$$

if  $\left[ \frac{v_m}{(N_r K_s)} \right] + e^{-\alpha \psi_0} > 0$

$$\psi(z_m) = -\frac{1}{\alpha} \ln \left( -\exp \left\{ \ln \left[ \frac{v_m}{(N_r K_s)} \right] + e^{-\alpha \psi_0} \right\} - \alpha \omega^2 \rho_w z_m \left[ r_0 - \left( \frac{z_m}{2} \right) \right] - \frac{v_m}{N_r K_s} \right)$$

if  $\left[ \frac{v_m}{(N_r K_s)} \right] + e^{-\alpha \psi_0} > 0$

where  $\psi_0$  is the matric potential at the outflow face of the centrifuge sample, and  $N_r$  is a function of  $z_m$ .  $z_m$  is the distance from the datum at the base of the specimen,  $K_s$  is the saturated hydraulic conductivity of the sample,  $\alpha$  is a fitting parameter and  $v_m$  is the water velocity in the direction of the axis of rotation.

The theoretical  $\psi$  profile of a chalk sample under steady-state conditions was obtained using equation (4) and the results were compared with the  $\psi$  profile obtained using equation (3). The results are shown in Figure 4. The  $\psi$  profile was calculated for a saturated lower boundary sample, and a known imposed surface infiltration velocity. The parameter  $\alpha$  is related to the inverse of the air entry pressure of the chalk, which is equal to  $0.005 \text{ kPa}^{-1}$ , estimating the chalk air entry pressure to be equal to  $-200 \text{ kPa}$  (Ireson 2008). The height at any point in the sample,  $z_m$ , is normalized by the sample height  $L_m$  (120 mm). Calculating the  $\psi$  profile using equation (3) leads to a positive matric potential value, as the sample is at steady-state flow condition and it is already saturated. However, using equation (4) leads to a negative matric potential, where  $\psi$  has a negative value, below saturation level, thus the results are negative. However, this does not influence the shape of the curve. The equilibrium  $\psi$  profile (equation (3)) has a more linear shape compared with the steady-state  $\psi$  profile (equation (4)). Calculation spreadsheets are available in the Supplementary material. The steady-state profile infiltration reaches values that remain relatively constant from the upper portion of the sample. The upper portion does show a slight gradient, but it is assumed constant for this study.

The pattern of the steady-state  $\psi$  profile, which shows a nearly constant  $\psi$  in the upper part of the sample, was a significant aspect of the steady-state infiltration under high centrifuge acceleration, and it was important in designing the instrument layout. In the upper part of the sample, where the  $Z_m/L_m$  is above 0.3, the  $\psi$  value is constant, but below this part the  $\psi$  value is not constant and changes linearly. Similarly, during steady-state flow,  $\theta$  should be relatively constant in the upper part of the sample.

The effect of the centrifugal acceleration ( $N_r$ ) on the  $\psi$  profile, when using constant  $v_m$ , is shown in Figure 5. The theoretical results have been calculated using equation (4). Results show that with increasing  $N_r$  the uniformity of the  $\psi$  profile increases as well, mainly in the upper portion of the sample. The  $\psi$  value along with the sample profile during steady-state infiltration was less sensitive to the variations of  $N_r$ , but with a lower  $N_r$ , the results became closer to a linear change along the length of the sample rather than a constant value.

The effect of different infiltration rates used in equation (4) on the  $\psi$  profile, with constant  $N_r$ , is shown in Figure 6. The figure illustrates that the  $\psi$  profile is sensitive to the water inflow rates used in steady-state tests. A higher inflow of water leads to a uniform  $\psi$

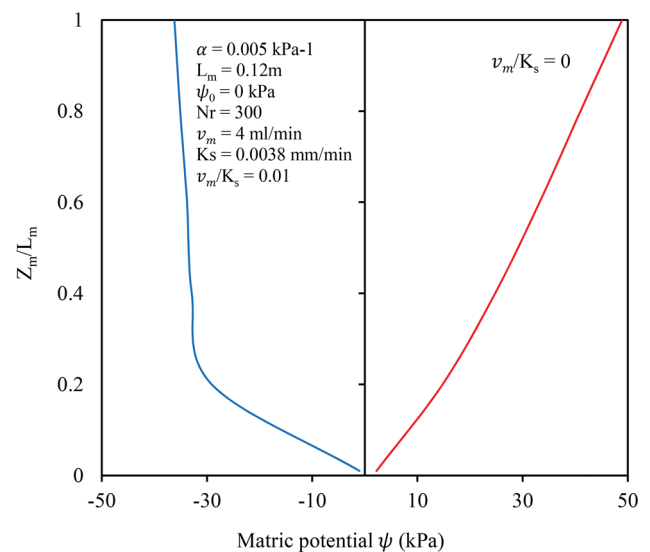
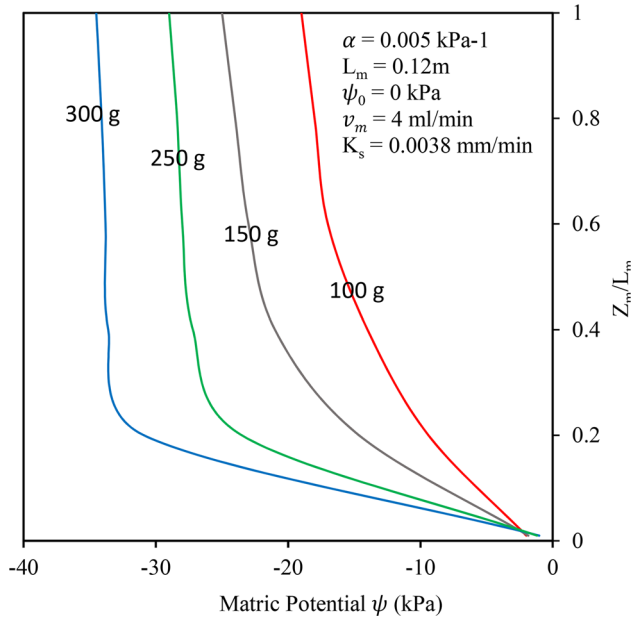


Fig. 4. Theoretical matric potential ( $\psi$ ) profiles in the centrifuge showing a comparison between equilibrium (equation (3); right) and steady-state condition (equation (4); left).

## Hydraulic properties of chalk



**Fig. 5.** Theoretical matric potential ( $\psi$ ) profiles using equation (3) showing a comparison between steady-state flows at different values of  $N_r$ .

profile.  $\psi$  at the base of the sample was observed to be non-uniform; this agrees with observations by *Avanzi et al. (2004)* and *Zornberg and McCartney (2010)* during centrifuge tests with unsaturated soil.

The flow of water under increased gravity is driven by the total hydraulic gradient, in the same way as under normal gravity. The total hydraulic head is the sum of the matric potential head, elevation head, velocity head and osmotic head. The velocity head during the steady state is very small (less than 0.01–0.05 mm) so it is neglected in this study. The osmotic pressure does not change with change in water content except under very dry conditions (*Villar 2002*), thus the osmotic gradient is neglected during water flow in the sample. The flow in the sample is driven by the hydraulic gradient and is representative of subsurface flow in the field, as the block of chalk used in the centrifuge models (height 120 mm, scale

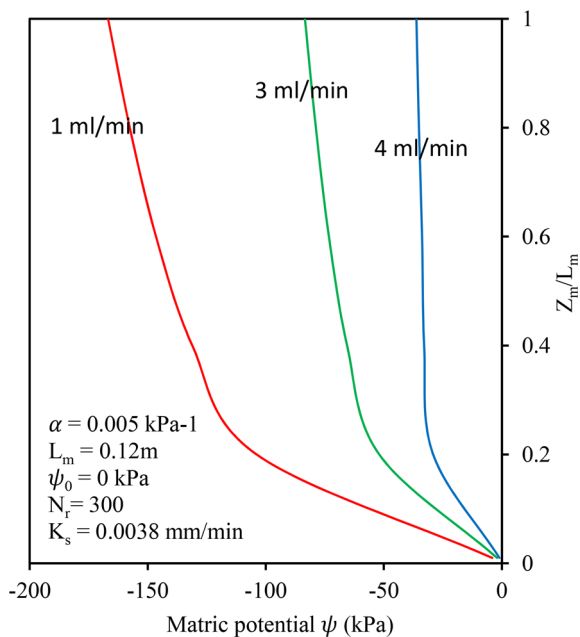


**Fig. 6.** Theoretical matric potential ( $\psi$ ) profiles in a centrifuge test showing a comparison between steady-state flows with a different rate of inflow.

factor 1/300) represents a 36 m high column of chalk in the field. The simulated depth conditions are typical of the chalk aquifer, where the unsaturated zone can reach up to 80 m thickness on interfluvial (*Rutter et al. 2012*). Therefore, the stresses in the chalk sample will be the same as in the field up to 36 m below ground, leading to the same flow distribution between fractures and matrix in model and field. *Schofield (1980)*, *Goodings (1985)* and *Taylor (1987)* agreed that the hydraulic permeability is independent of the increased gravity in a centrifuge model.

The centrifuge technique developed in this study was intended to allow air to move freely from the base of the sample, so the pore air pressure is assumed to be atmospheric ( $P_a = 0$ ). According to this assumption the hydraulic head ( $h_m$ ) in the centrifuge can be given as follows:

$$h_m = -\frac{\omega^2}{2g}(r_0 - z_m)^2 - \frac{\psi}{\rho_w g}. \quad (5)$$

The first term on the right-hand side of the equation represents the centrifuge elevation head and the second term represents the matric potential head. The first term in equation (5) has been used to calculate the elevation head in the centrifuge and compare the results with the matric potential head calculated using equation (4). The results are shown in Figure 7. The figure shows that the elevation head under centrifuge conditions is much greater than the matric potential head. The matric potential head approaches zero at the bottom of the sample, near the outflow boundary. The result indicates that the centrifuge method is dominated by the elevation head, which according to *Zornberg and McCartney (2010)* dominates the total head gradient in the upper portion of the sample under accelerated gravity.

The distribution of the total head and change in elevation ( $z_m$ ) through the sample under the centrifuge method during steady-state conditions can be combined with Darcy's law to estimate unsaturated hydraulic conductivity  $K_{(\psi, \theta)}$  as follows:

$$k_{(\psi, \theta)} = \frac{v_m}{(\omega^2/g)(r_0 - z_m) - [1/(\rho_w g)](d\psi/dz_m)} \quad (6)$$

where  $v_m$  is the steady-state discharge velocity, which is equal to the infiltration rate divided by the cross-sectional area of the sample surface. The denominator represents the total hydraulic gradient under the centrifuge condition.

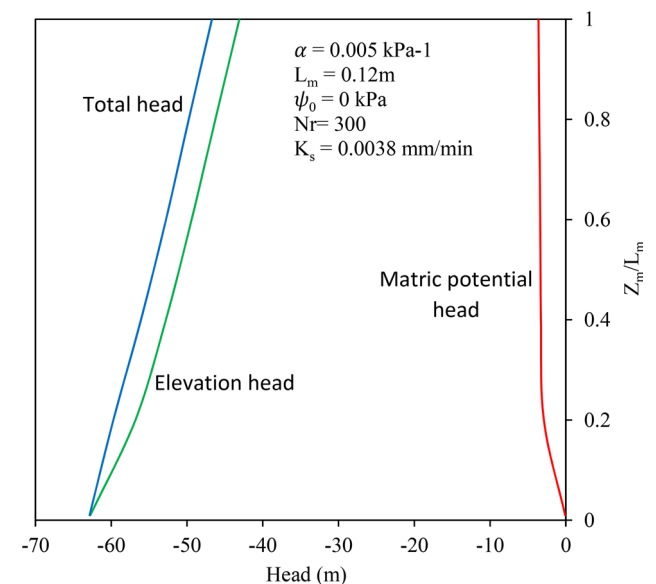


**Fig. 7.** Theoretical head profiles during steady-state flow in the centrifuge.

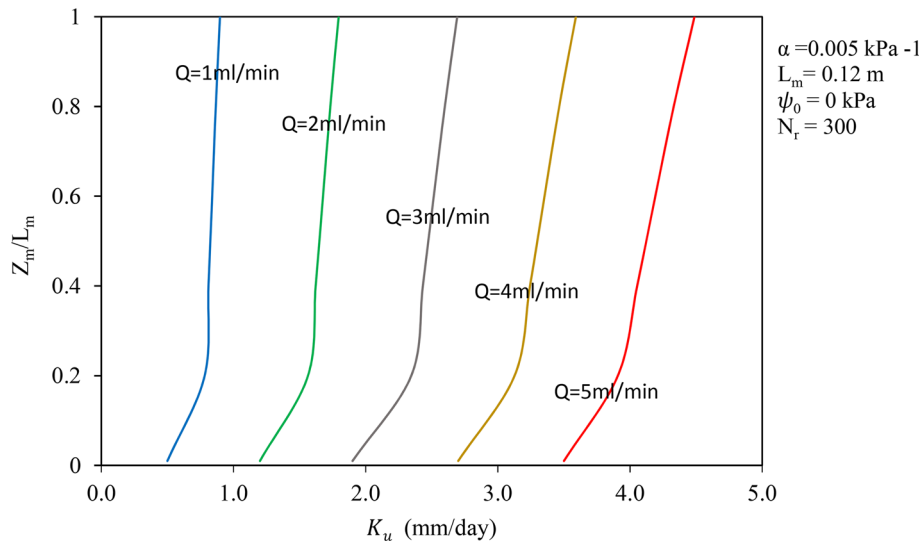


**Fig. 8.** Theoretical  $K_u$  profile on the chalk sample during steady-state infiltration with a variation of inflow discharge.

Centrifugal acceleration is given by the factor  $N_r$  (acceleration =  $N_r g$ ) so that the physical behaviour for a sample scaled  $1/N_r$  under centrifuge conditions would be the same as the natural condition for a full size prototype. The samples were selected to avoid visible heterogeneities, with the aim of characterizing the matrix hydraulic properties. In this study, the hydraulic conductivity, matric potential and volumetric water content will always be equal to the coefficient of proportionality between the applied hydraulic gradient and the flow rate, regardless of gravity. Thus, the results are not scaled in this study. [Tan and Scott \(1985\)](#) found that hydraulic conductivity is not scaled under centrifugal acceleration. The distribution of the theoretical hydraulic conductivity (using equation (6)) through the chalk sample is shown in [Figure 8](#). In the figure, only the rate of inflow is changed, and all other parameters remain constant. The figure shows that the hydraulic conductivity is constant in the upper portion of the sample in the same way as the other parameters.

### Measured hydraulic properties of the chalk

The centrifuge speed ( $\omega$ ) and the inflow rate ( $Q$ ) are the main variables that can be controlled in the centrifuge method during infiltration tests. The procedure of the centrifuge test involves selecting several controlled variables. However, from the previous sections, several theoretical results have been obtained, which show the best situations that attain a steady-state condition. These are a constant centrifuge acceleration factor ( $N_r$ ) of 300 and a variable inflow rate starting from 2 ml min<sup>-1</sup>. The variables that needed to be measured during the steady-state infiltration to calculate  $K_u$  and the SMC curve are  $\psi$ ,  $\theta$  and the outflow rate (to ensure that the steady-state condition has been attained). These parameters characterize steady-state infiltration in the centrifuge. The wpt sensors were located at constant height on the upper portion of the sample where the measurements were predicted to remain constant ([Avanzi \*et al.\*](#)

[2004](#); [Zornberg and McCartney 2010](#)). The water content was measured from the upper part of the sample using the FDR technique, which gives a good estimation of the  $\theta$  of the upper portion of the chalk sample. This method of measuring  $\theta$  was also used by [Zornberg and McCartney \(2010\)](#) using an FDR waveguide from the upper portion of a soil sample. The  $\theta$  measured with the FDR can be used to find the hydraulic properties in the chalk sample, with the  $\psi$  from three locations of the sample, mainly from the constant steady-state portion ( $z_m = 30, 60$  and  $90$  mm). Within this portion, the matric potential can be measured directly from the water pressure transducers, which were located at heights of 30, 60 and 90 mm from the base of the chalk sample ([Fig. 3](#)). [Table 1](#) shows the tests undertaken using the centrifuge permeameter for the chalk samples. Full results and calculations from the tests are available at <https://researchdata.brighton.ac.uk/id/eprint/283/>.

The value of  $K_u$  can be calculated directly from the data obtained from the centrifuge using [equation \(6\)](#), using  $v_m$  as a controlled variable, along with the  $\psi$  gradient  $d\psi/dz_m$ , which is determined using the  $\psi$  measured value from the chalk sample during the in-flight conditions.  $K_u$  is a function of  $z_m$  because both elevation and the matric potential gradient in [equation \(6\)](#) are a function of  $z_m$ .  $K_u$  has been calculated theoretically using [equation \(6\)](#) and supposing a matric potential of zero. This result was compared with the result obtained from the centrifuge experiment. Selection of the controlled variable of water inflow will affect the range of the results and the test time. In this study the hydraulic characteristics of the unsaturated chalk samples were measured using a constant centrifuge speed and varying inflow rate.

### Infiltration rate

The amount of water used in each test is significant in determining  $K_u$  values. It is also necessary to reach a steady-state condition to

**Table 1.** Conditions of tests carried out using the centrifuge permeameter

| No. | Test name | Purpose                       | Sample condition | Inflow rate (ml min <sup>-1</sup> ) | Duration (h:min) |
|-----|-----------|-------------------------------|------------------|-------------------------------------|------------------|
| 1   | T1        | Measure $K_u$                 | Wetting          | 2                                   | 7:30             |
| 2   | T2        | Measure $K_u$                 | Wetting          | 4                                   | 5                |
| 3   | T3        | Measure $K_u$                 | Draining         | 0                                   | 3                |
| 4   | T4        | Draw SMC curve, measure $K_u$ | Draining         | 0                                   | 4                |
| 5   | T5        | Draw SMC curve, measure $K_u$ | Wetting          | 5                                   | 4                |
| 6   | T6        | Draw SMC curve, measure $K_u$ | Draining         | 0                                   | 9:30             |
| 7   | T7        | Draw SMC curve, measure $K_u$ | Wetting          | 4                                   | 6                |
| 8   | T8        | Draw SMC curve, measure $K_u$ | Wetting          | 4                                   | 5:30             |

## Hydraulic properties of chalk

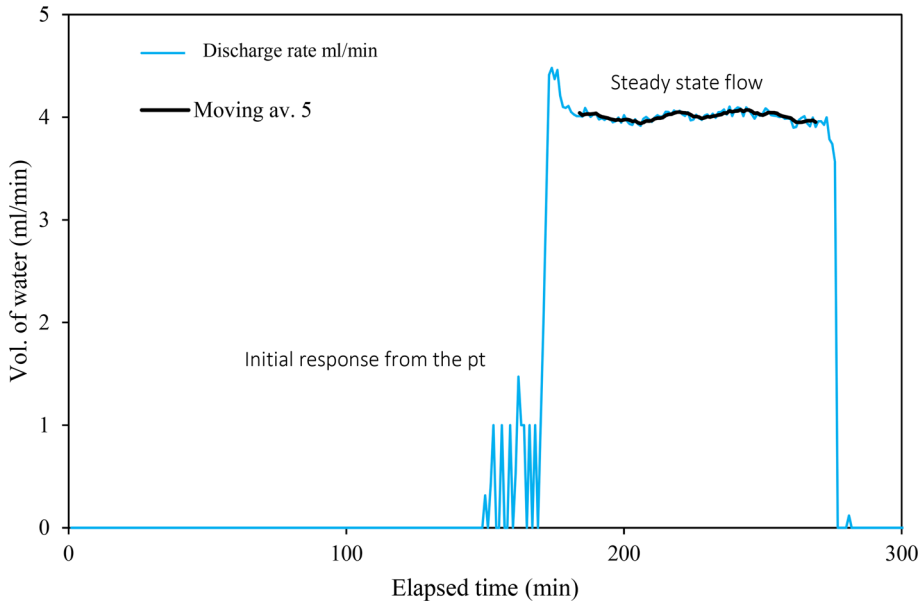


Fig. 9. Discharge rate (in  $\text{ml min}^{-1}$ ) for test T2 showing a steady-state condition.

calculate  $K_u$ . When water is added to the top of each sample in the wetting test, water starts to fill the matrix of the chalk sample. Then at a certain level of saturation water begins to pass through the sample. The amount of time required for this depends on the infiltration rate. Figure 9 shows the volume of water passing through the sample in the T2 test using  $4 \text{ ml min}^{-1}$  infiltration rate. The chalk sample was dry at the start of the test and it took 150 min for water to pass through the sample. After 180 min water started to flow out at a constant rate where the infiltration and discharge became equal. At this point, the flow reached a steady-state condition. The time and duration of each test depended on the time required to reach steady-state conditions; a test using a low infiltration rate generally required a longer time to reach steady-state conditions.

### Steady-state conditions

The matric potential ( $\psi$ ) profiles defined using data recorded from three wpts once steady-state conditions were established should record constant values within a single test. Figure 10 shows the steady-state condition during the wetting process of the three pressure transducers that were located at three sample heights ( $z_m$ ). Each reached a steady-state condition at different matric potential ( $\psi$ ) values after 100 min of centrifuge testing. Also, the volumetric

water content ( $\theta$ ) was measured with matric potential ( $\psi$ ), and showed a constant value during steady-state flow conditions. There is little change in the matric potential ( $\psi$ ) recorded at  $z_m = 30 \text{ mm}$ . This is because it is close to the lower portion of the chalk sample. This situation was observed in the theoretical matric potential calculation where the matric potential ( $\psi$ ) is less stable in the lower part of the sample.

Figure 11 shows the total hydraulic head during a centrifuge test. The total hydraulic head was calculated using equation (5), and the elevation head was calculated using the first term on the right-hand side of the same equation. The potential head was calculated using equation (4). The matric potential is close to zero (Fig. 10), but the elevation head was higher. In the same way as for  $\psi$  and  $\theta$ , the hydraulic head is relatively constant during the steady-state condition. The elevation head is much higher than the potential head in the centrifuge technique; this condition is observed in both theoretical and practical use of the centrifuge for the chalk samples.

### Measurement of unsaturated hydraulic conductivity ( $K_u$ )

Results of the unsaturated hydraulic conductivity ( $K_u$ ) measured in each test are shown in Figure 12a and b. A decrease in  $K_u$  value is observed with a decrease in matric potential ( $\psi$ ). In test T1, the matric potential ( $\psi$ ) is equal to  $-14 \text{ kPa}$  and the unsaturated

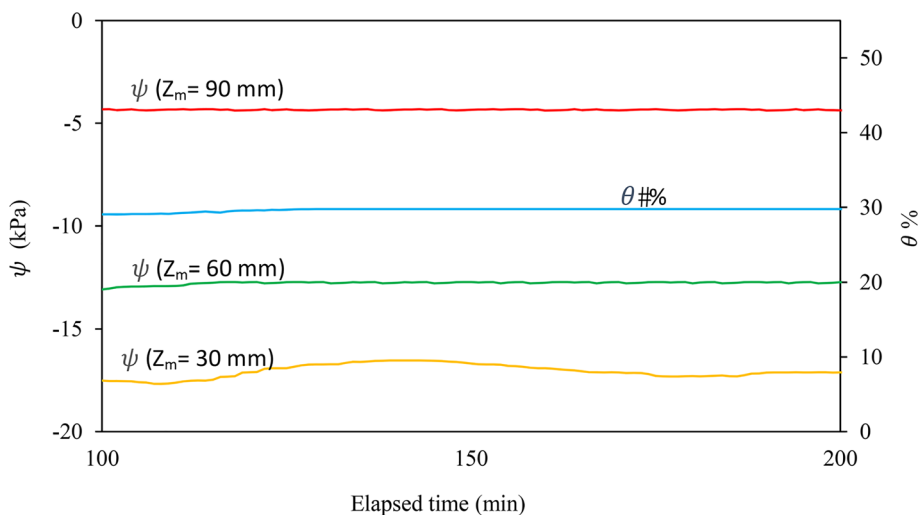
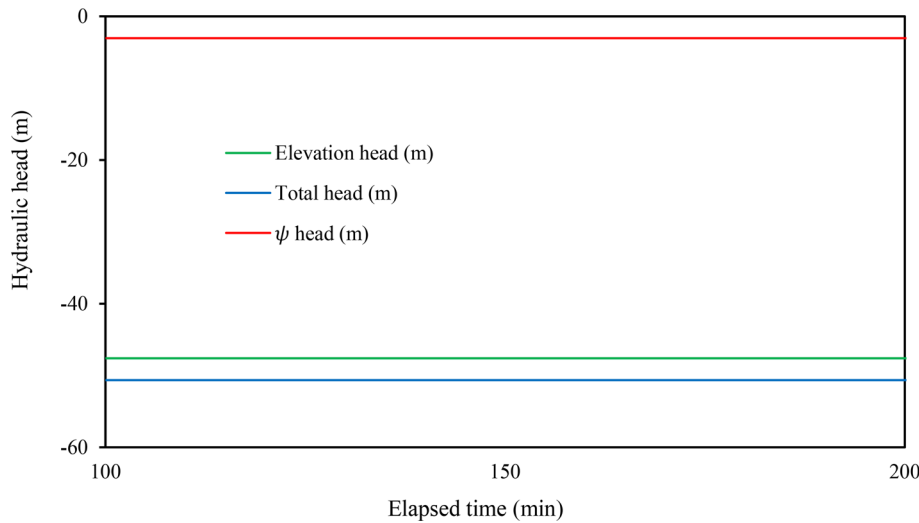


Fig. 10. Matric potential ( $\psi$ ) and volumetric water content ( $\theta$ ) results in the steady-state condition for the wetting test (T5).



**Fig. 11.** Hydraulic head during steady-state condition showing matric potential, elevation head and total head for test T5.

hydraulic conductivity ( $K_u$ ) is equal to  $1.4 \text{ mm day}^{-1}$ . In contrast, the unsaturated hydraulic conductivity ( $K_u$ ) rises to  $4 \text{ mm day}^{-1}$  when the matric potential ( $\psi$ ) increases to  $-4 \text{ kPa}$  in test T5. With decreasing matric potential ( $\psi$ ) to below  $-40 \text{ kPa}$  in tests T4 and T6, unsaturated hydraulic conductivity ( $K_u$ ) decreases to about  $0.069 \text{ mm day}^{-1}$ . This value is the minimum that can be measured using the wpt in the centrifuge permeameter at this level. When the matric potential is  $-50 \text{ kPa}$  and below, only the matrix contributes to flow and almost all fracture and fissures are drained. It is not easy to measure unsaturated hydraulic conductivity ( $K_u$ ) below this level, because the flow in the chalk matrix is very slow.

#### Soil moisture characteristic curve

A gradual decrease in porewater content leads to a decrease in total pore pressure, which is a result of progressive emptying of fractures and larger pore space until only the very narrow pores retain water. This relationship between water content ( $\theta$ ) and pore pressure ( $\psi$ ) is known as the soil moisture characteristic (SMC) curve. Values of  $\psi$  and  $\theta$  obtained from the centrifuge experiments were used to plot SMC curves. The curves are important in understanding the way

water moves and distributes in the unsaturated zone. Data obtained from the centrifuge tests were used to build SMC curves in both wetting and draining tests, so the influence of the fractures and hysteresis is also shown. Hysteresis is a common hydraulic feature occurring in the unsaturated chalk (Molyneux 2012), in which, at a given  $\psi$ , the  $\theta$  on the draining curve is always higher than on the wetting curve.

Wetting and draining tests were undertaken to investigate the nature of the SMC curve under the two conditions. Also, these two conditions demonstrate the hysteresis behaviour of the chalk during the draining and wetting process. Typical results from an intact chalk sample are shown in Figure 13. Both  $\psi$  and  $\theta$  were recorded simultaneously during in-flight conditions, allowing construction of the SMC curve.

Details from the typical wetting and draining SMC curve (Fig. 13) indicate the presence of three pressure zones: the low-pressure zone, intermediate-pressure zone and high-pressure zone. These zones may relate to the mechanism of water flow in the chalk unsaturated zone, which in turn may relate to the flow process that occurs through matrix and fracture contribution in the chalk. The low negative pressure zone (Lnp) is the zone where water mainly

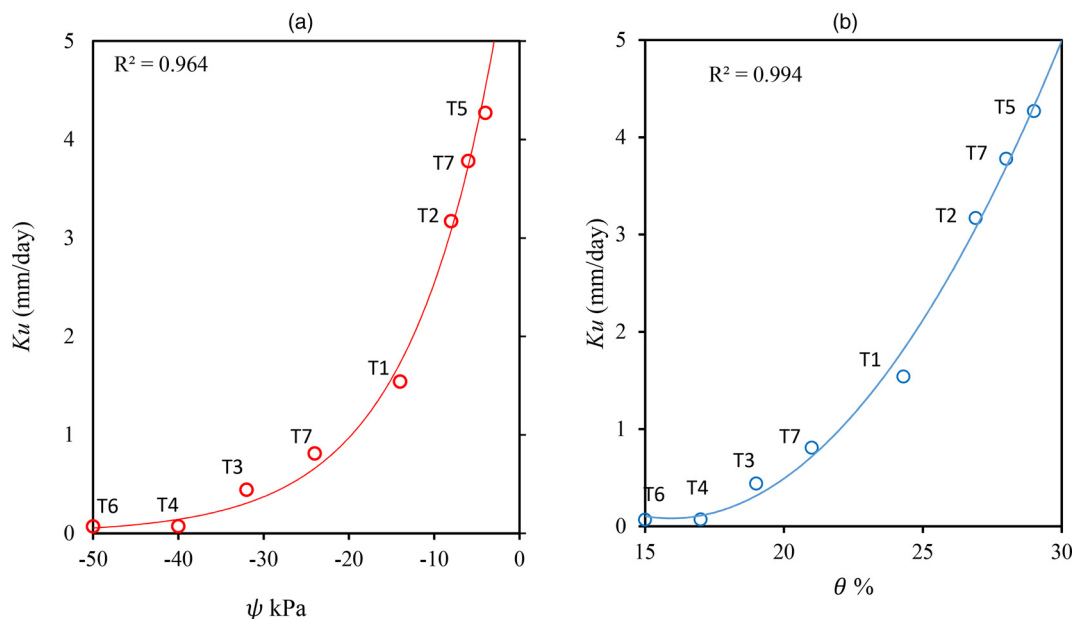


**Fig. 12.** Unsaturated hydraulic conductivity ( $K_u$ ) results from the centrifuge tests comparing  $\psi$  (a) and  $\theta$  (b) values. The lines (red and blue) are the best fit using an exponential function.

## Hydraulic properties of chalk

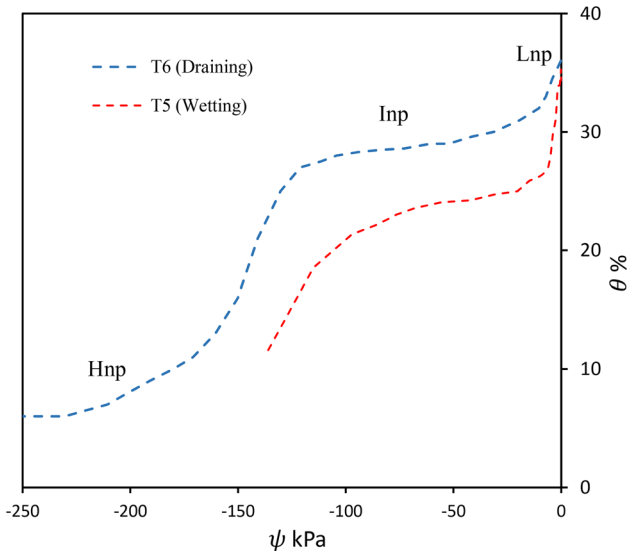


**Fig. 13.** SMC curve for the wetting (T5) and draining (T6) process of an intact chalk sample,  $\psi$  from wpt2. These tests demonstrate the hysteresis behaviour. Hnp, high negative pressure; Inp, intermediate negative pressure; Lnp, low negative pressure.

starts to flow. This zone begins when the  $\psi$  rises above  $-5$  kPa and  $\theta$  to above 30% in the case of the draining process and 26% in the case of the wetting process. In this zone, both matrix and fractures are inferred to be conducting water. The intermediate negative pressure zone (Inp) is the zone where the fractures are dry, and water is held in the matrix of the chalk, but the  $\psi$  remains above the air entry value. In this zone, the  $\psi$  reaches  $-100$  kPa and  $\theta$  reaches 26% for the draining process and 18% for the wetting process. In this zone, flow is inferred to mainly occur in the matrix of the chalk and the fractures are not contributing to the flow process. In the high negative pressure zone (Hnp), the matrix starts to desaturate and  $\psi$  falls below air entry pressure. The results from the SMC curves are similar to the SMC curve found by Ireson (2008), whereas the typical SMC curve found by Molyneux (2012) was extended to higher  $\psi$  ( $-1000$  kPa).

Details of calculations and test results are available at <https://researchdata.brighton.ac.uk/id/eprint/283/>.

## Evaluation of the results

### The SMC related to the BC, VG and KS models

The  $\psi$ - $\theta$  values measured during the centrifuge test in the chalk samples during tests T5 (wetting) and T6 (draining) were evaluated using the Brooks and Corey (BC; Brooks and Corey 1964), Van Genuchten (VG; Van Genuchten 1980) and Kosugi (KS; Kosugi 1996) models. An SWRC fit program developed by Seki (2018) was used to evaluate the BC, VG and KS models. The parameters used for this evaluation are shown in Table 2. Figure 14 shows the results of tests T5 and T6 with the BC, VG and KS models. Generally, the curves from the two tests are very similar to the BC, VG and KS models. The best match is where the chalk is close to saturation, mainly when all the pore space and fissures are inferred to contribute to conducting water, but with higher  $\psi$  and decreasing matrix saturation  $\theta$  the measured data do not match the models quite as well. In the chalk, the pore size distribution is not well understood because of the presence of microfractures in the system. Employing the bundle of cylindrical capillaries (BCC) model, the water content of the pores decreases or increases progressively during the draining and wetting process, whereas at higher  $\psi$  only smaller pores are left saturated. This situation may cause the mismatch at this level ( $\psi$

**Table 2.** Equations and parameters used to evaluate the BC, VG and KS models

| Model           | Equation   | Parameters   | $R^2$ |
|-----------------|--|--|-------|
| Brook and Corey | $S_e = \left(\frac{\psi_s}{\psi}\right)^\lambda$ when $\psi < \psi_s$<br>$S_e = 1$ when $\psi \geq \psi_s$ | $\psi_s = -208$<br>$\lambda = 0.14$                  | 0.93  |
| Van Genuchten   | $s_e = \left[\frac{1}{1 +  \alpha\psi ^n}\right]^m$  | $\alpha = 0.04$<br>$n = 26.3$<br>$m = 0.11$          | 0.96  |
| Kosugi          | $S_e = Q \left[ \ln \left( \frac{\psi}{\psi_0} \right) / \sigma - \sigma \right]$                          | $Q = 0.0015$<br>$\psi_0 = -249.7$<br>$\sigma = 0.73$ | 0.96  |

$\psi_s$  is air entry pressure (kPa),  $\lambda$  is the Brook–Corey exponent (dimensionless),  $\alpha$  and  $n$  are parameters,  $\psi_0$  is the matric potential at the outflow face of the centrifuged sample (kPa),  $\sigma$  is the standard deviation of  $\ln(\psi/\psi_0)$ ,  $Q$  is the complementary normal distribution function.

between  $-30$  and  $-120$  kPa in the draining process and between  $-30$  and  $-100$  kPa in the wetting process). When the chalk sample become drier ( $\psi$  below  $-120$  kPa) the KS and VG models match the recorded data well, but the BC model does not match the recorded data, notably during the draining process, showing a higher water content ( $\theta$ ).

### Comparison of measured $K_u$ with predicted $K_u$

The  $K_u$  values calculated during steady-state conditions from all the centrifuge tests (T1–T8) were compared with the predicted  $K_u$  values calculated using equation (6), using different infiltration rates and  $\psi$  values predicted from equation (4). The measured and predicted  $K_u$  values are related to changing  $\psi$  and  $\theta$  and compared with each other in Figure 15a and b. Mostly, the predicted  $K_u$  values follow the same trend as the measured  $K_u$  but do not match exactly. The predicted  $K_u$  calculated using equation (6) underestimates  $K_u$  value for  $\psi$  by less than  $-20$  kPa, and overestimates  $\theta$ . The poor match of the predicted  $K_u$  to measured  $K_u$  was also observed by McCartney and Zornberg (2010) and Khaleel *et al.* (1995) on compacted soil. The poor match of the measured and predicted  $K_u$  values emphasizes the importance of determining  $K_u$  experimentally rather than relying on predicted relationships. The  $K_u$  of the chalk samples measured using the centrifuge technique provides enough data to characterize the relationship of  $K_u$  to  $\psi$  and  $\theta$ . From the extension of the curve of the measured  $K_u$ , it is possible to estimate the saturated matrix hydraulic conductivity ( $K_{sm}$ ) as about

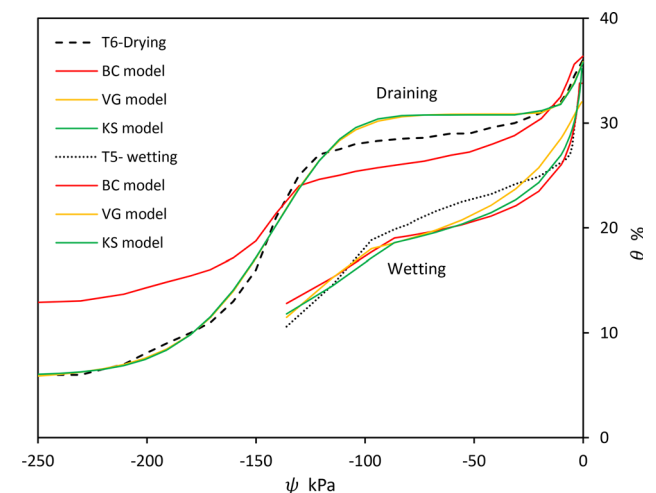


**Fig. 14.** Soil moisture characteristic (SMC) curve during tests T5 and T6 evaluated using the BC, VG and KS models.

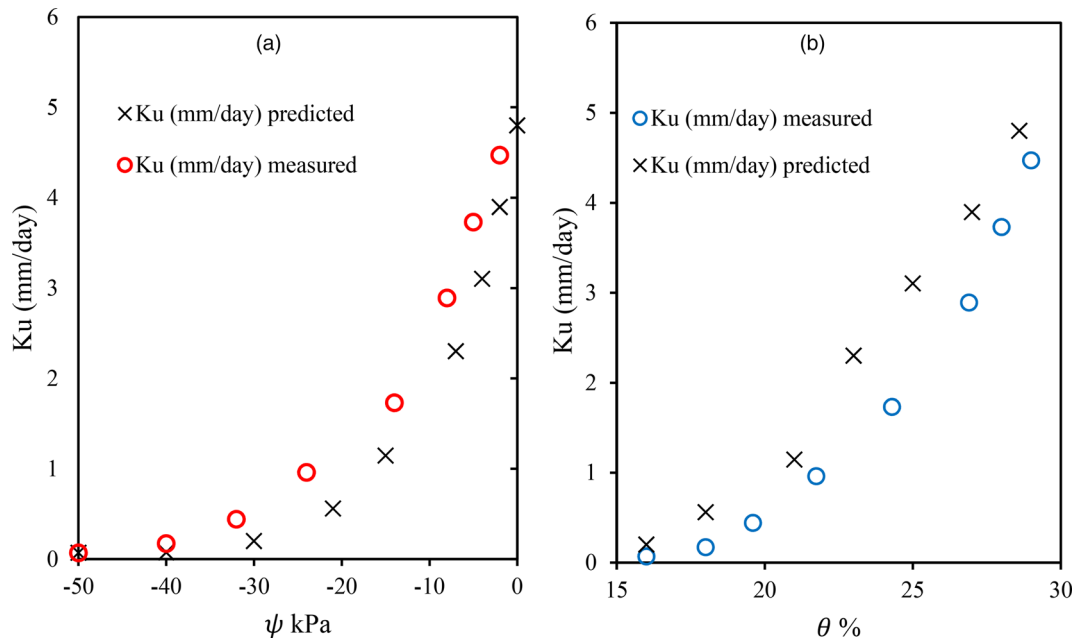


Fig. 15. Comparison of measured and predicted  $K_u$  related to  $\psi$  (a) and  $\theta$  (b) from all the tests.

6 mm day<sup>-1</sup>, whereas the predicted measurement is 4.8 mm day<sup>-1</sup>. Molyneux (2012) measured mean saturated hydraulic conductivities of South Downs samples of the Lewes Chalk of 1.0 mm day<sup>-1</sup> with a range of 0.01–8.3 mm day<sup>-1</sup> (52 samples) and of the Seaford Chalk of 4 mm day<sup>-1</sup> with a range of 1.8–16 mm day<sup>-1</sup> (23 samples). Our results, extrapolated to a matric potential of 0 kPa, are therefore entirely consistent with previous measurements of hydraulic conductivity.

The  $K_u$  results from the tests represent the flow-through test T5 where flow occurs at  $\psi = -4$  kPa. In this test, there may be a contribution from fracture flow. However, the  $K_u$  graph in Figure 15 shows that there is a gradual increase in  $K_u$  with an increase in both  $\psi$  and  $\theta$ . This indicates that there is the gradual filling of pore space followed by the fractures starting from the smallest pores. Most previous work followed the assumption that fractures hold and transmit water at a  $-5$  kPa threshold. This idea was first presented by Wellings (1984) for flow in the chalk unsaturated zone. Nevertheless, the data obtained from the centrifuge tests ( $K_u$ – $\psi$ ) and ( $K_u$ – $\theta$ ) show that instead of the presence of an inflection point, there is a more gradual increase in  $K_u$  reflecting the change in both  $\psi$  and  $\theta$ . This demonstrates that fractures do not suddenly fill with water at a threshold value of  $\psi$ , but behave as large pores, filling gradually with water. Moreover, during recharge periods, the matrix starts to conduct water, followed by small fractures and then larger ones. Thus, saturation occurs gradually and the fractures function as a larger-scale pore matrix in conducting water.

## Conclusion

In this study, the hydraulic characteristics of chalk were determined using rapid centrifuge tests. The data matched the predictions from theoretical calculations. The theoretical background of unsaturated flow under centrifuge conditions was presented, which allowed the prediction of the matric potential ( $\psi$ ) and volumetric water content ( $\theta$ ) under centrifuge conditions. The measured matric potential ( $\psi$ ) profile for the chalk sample is consistent with predicted values during steady-state infiltration. The matric potential ( $\psi$ ) profiles measured in the centrifuge using water pressure transducers (wpt) indicate that  $\psi$  and  $\theta$  are constant in the chalk sample, particularly in the upper portion of the sample during steady-state conditions, in both wetting and draining tests. At higher acceleration the matric

potential ( $\psi$ ) profile was observed to be more uniform, for higher infiltration rates to reach steady-state conditions.

Using different infiltration rates in the centrifuge allowed much faster measurement of unsaturated hydraulic conductivity ( $K_u$ ) at different water contents compared with previously reported techniques. The resulting  $K_u$  values varied according to the infiltration rate, matric potential and volumetric water content values. The  $K_u$  values varied from 4.27 mm day<sup>-1</sup> using 4 ml min<sup>-1</sup> of water in test T5 to 1.54 mm day<sup>-1</sup> using 2 ml min<sup>-1</sup> of water during test T1. Also, there is gradual increase of  $K_u$  value with increase in both  $\psi$  and  $\theta$ . Generally, the  $K_u$  values are dependent on the amount of infiltrated water,  $\psi$  and  $\theta$  because of different saturation levels in the chalk. The test results demonstrate that there is a progressive increase in unsaturated hydraulic conductivity ( $K_u$ ) as the smaller pores fill, implying that there is no single threshold in  $\psi$  for the initiation of fracture flow, and that the fracture system essentially behaves as large pores.

The data from the tests allow the construction of SMC curves, showing hysteresis in the chalk samples. The SMC curve shows a nonlinear relationship between  $\psi$  and  $\theta$  with three zones: a low negative pressure zone, intermediate negative pressure zone and high negative pressure zone. In the low negative pressure zone, both matrix and fractures are inferred to contribute to flow and recharge through the chalk unsaturated zone. In the intermediate negative pressure zone, only matrix contributes to flow and the fractures are dry. Finally, in the high negative pressure zone, there is no flow and water is strongly bound in the smallest pores; this is sometimes called the air entry zone.

The soil moisture characteristic (SMC) curves and  $K_u$  values from the experiments were compared with the BC, VG and KS models and the  $K_u$  predicted values. In general, it is noted that the SMC curve drawn from the tests matches the VG and KS models. The measured  $K_u$  values did not match the predicted results but followed the same trends. Comparing the measured  $K_u$  with literature data indicated good repeatability of the results, but with less time required to complete measurements. Overall, the geotechnical centrifuge was successfully used as a new tool to study hydraulic characteristics of the chalk. The technique could be applied to determination of unsaturated hydraulic properties across a range of materials, and the properties determined used to support improved models of unsaturated zone flow.

## Hydraulic properties of chalk

**Acknowledgement** This work was undertaken as part of PhD study at the University of Brighton, all the laboratory work was performed at the University. We thank the anonymous referees for constructive comments which have helped to improve this manuscript.

**Author contributions** PA-J: data curation (lead), formal analysis (lead), funding acquisition (lead), investigation (lead), methodology (lead), writing – original draft (lead), writing – review & editing (equal); MS: supervision (lead), validation (lead), visualization (lead), writing – review & editing (lead); FG: supervision (equal), validation (equal), writing – review & editing (equal)

**Funding** This research received no specific grant from any funding agency in the public, commercial or not-for-profit sectors.

**Competing interests** The authors declare that they have no known competing financial interests or personal relationships that could have appeared to influence the work reported in this paper.

**Data availability** The data that support the findings of this study are available from the University of Brighton, but restrictions apply to the availability of these data, which were used under licence for the current study, and so are not publicly available. Data are however available from the authors upon reasonable request and with permission of Prof. Martin Smith.

Scientific editing by Fleur Loveridge; Mike Long

## References

- Avanzi, E.D., Zornberg, J.G. and Cabral, A.R. 2004. Suction profiles and scale factors for unsaturated flow under increased gravitational field. *Soils and Foundations*, **44**, 79–89, [https://doi.org/10.3208/sandf.44.3\\_79](https://doi.org/10.3208/sandf.44.3_79)
- Briggs, L.J. and McLane, J.W. 1910. Moisture equivalent determinations and their application. *Agronomy Journal*, **2**, 138–147, <https://doi.org/10.2134/agronj1910.00021962000200010024x>
- Brooks, R.H. and Corey, A.T. 1964. Hydraulic properties of porous media and their relation to drainage design. *Transactions of the ASAE*, **7**, 26–0028, <https://doi.org/10.13031/2013.40684>
- Conca, J. and Wright, J. 1992. Flow and diffusion in unsaturated gravel, soil and whole rock. *Applied Hydrogeology*, **1**, 5–24, <https://doi.org/10.1007/PL00010963>
- Downing, R.A., Price, M. and Jones, G.P. (eds) 1993. *The Hydrogeology of the Chalk of North-West Europe*. Clarendon, Oxford.
- Feng, Z. and Yin, Y. 2014. Geotechnical centrifuge modelling for rock slope failure: a brief overview. In: Sassa, K., Canuit, P. and Yin, Y. (eds) *Landslide Science for a Safer Environment. Volume 2: Methods of Landslide Studies*, Springer, 39–43, [https://doi.org/10.1007/978-3-319-05050-8\\_7](https://doi.org/10.1007/978-3-319-05050-8_7)
- Gallagher, A.J., Rutter, H.K., Buckley, D.K. and Molyneux, I. 2012. Lithostratigraphic controls on recharge to the Chalk aquifer of Southern England. *Quarterly Journal of Engineering Geology and Hydrogeology*, **45**, 161–172, <https://doi.org/10.1144/1470-9236/09-048>
- Gardner, R. 1937. The method of measuring the capillary pressures in small core samples. *Soil Science*, **43**, 277–283, <https://doi.org/10.1097/00010694-193704000-00004>
- Gardner, C., Cooper, J., Wellings, S., Bell, J., Hodnett, M., Boyle, S. and Howard, M. 1990. Hydrology of the unsaturated zone of the chalk of south-east England. In: *Chalk*, Thomas Telford, London, 611–618.
- Goodings, D.J. 1985. Relationships for modelling water effects in geotechnical centrifuge models. In: Craig, W. (ed.) *Application of Centrifuge Modelling to Geotechnical Design: Proceedings of a Symposium on the Application of Centrifuge Modelling to Geotechnical Design*, 16–18 April 1984, Manchester. Balkema, Rotterdam, 1–24.
- Haria, A.H., Hodnett, M.G. and Johnson, A.C. 2003. Mechanisms of groundwater recharge and pesticide penetration to a chalk aquifer in southern England. *Journal of Hydrology*, **275**, 122–137, [https://doi.org/10.1016/S0022-1694\(03\)00017-9](https://doi.org/10.1016/S0022-1694(03)00017-9)
- Hiscock, K.M. and Bense, V.F. 2014. *Hydrogeology: Principles and Practice*, 2nd edn. Wiley, New York.
- Ireson, A.M. 2008. *Quantifying the Hydrological Processes Governing Flow in the Unsaturated Chalk*. PhD thesis, Imperial College London, University of London.
- Khaleel, R., Relyea, J.F. and Conca, J.L. 1995. Evaluation of van Genuchten–Mualem relationships to estimate unsaturated hydraulic conductivity at low water contents. *Water Resources Research*, **31**, 2659–2668, <https://doi.org/10.1029/95WR02309>
- Kirkham, M.B. 2014. *Principles of Soil and Plant Water Relations*. Academic Press, London.
- Kosugi, K. 1996. Lognormal distribution model for unsaturated soil hydraulic properties. *Water Resources Research*, **32**, 2697–2703, <https://doi.org/10.1029/96WR01776>
- Lal, R. 2017. *Encyclopedia of Soil Science*. CRC Press, Boca Raton, FL.
- Levy, L.C., Culligan, P.J. and Germaine, J.T. 2002. Use of the geotechnical centrifuge as a tool to model dense nonaqueous phase liquid migration in fractures. *Water Resources Research*, **38**, 34-1–34-12, <https://doi.org/10.1029/2001WR000660>
- Mathias, S., Butler, A., McIntyre, N. and Wheeler, H. 2005. The significance of flow in the matrix of the Chalk unsaturated zone. *Journal of Hydrology*, **310**, 62–77, <https://doi.org/10.1016/j.jhydrol.2004.12.009>
- McCartney, J.S. and Zornberg, J.G. 2010. Centrifuge permeameter for unsaturated soils. II: Measurement of the hydraulic characteristics of an unsaturated clay. *Journal of Geotechnical and Geoenvironmental Engineering*, **136**, 1064–1076, [https://doi.org/10.1061/\(ASCE\)GT.1943-5606.0000320](https://doi.org/10.1061/(ASCE)GT.1943-5606.0000320)
- Molyneux, I. 2012. *Hydrogeological Characterisation of the Chalk: With Specific Reference to Unsaturated Zone Behaviour*. PhD thesis, University of Brighton.
- Moore, R. 1939. Water conduction from shallow water tables. *California Agriculture*, **12**, 383–426.
- Nimmo, J.R., Rubin, J. and Hammermeister, D. 1987. Unsaturated flow in a centrifugal field: measurement of hydraulic conductivity and testing of Darcy's law. *Water Resources Research*, **23**, 124–134, <https://doi.org/10.1029/WR023i001p00124>
- Or, D., Tuller, M. and Wraith, J.M. 2005. Soil water potential. *Encyclopedia of Soils in the Environment*, **3**, 270–277, <https://doi.org/10.1016/B0-12-348530-4/00364-7>
- Price, M., Bird, M.J. and Foster, S.S.D. 1976. Chalk pore size measurements and their significance. *Water Services*, **80**, 596–600.
- Price, M., Downing, R.A. and Edmunds, W.M. 1993. The Chalk as an aquifer. In: Downing, R.A., Price, M. and Jones, G.P. (eds) *The Hydrogeology of the Chalk of North-West Europe*. Oxford University Press, Oxford, 35–58.
- Richards, L.A. 1931. Capillary conduction of liquids through porous mediums. *Physics*, **1**, 318–333, <https://doi.org/10.1063/1.1745010>
- Rutter, H., Cooper, J.D., Pope, D. and Smith, M. 2012. New understanding of deep unsaturated zone controls on recharge in the Chalk: a case study near Patcham, SE England. *Quarterly Journal of Engineering Geology and Hydrogeology*, **45**, 487–495, <https://doi.org/10.1144/qjehg2011-010>
- Schofield, A.N. 1980. Cambridge geotechnical centrifuge operations. *Géotechnique*, **30**, 227–268, <https://doi.org/10.1680/geot.1980.30.3.227>
- Seki, K. 2018. SWRC Fit. Purl.org, <http://purl.org/net/swrc/> [retrieved 10 January 2022].
- Tan, T.S. and Scott, R. 1985. Centrifuge scaling considerations for fluid–particle systems. *Géotechnique*, **35**, 461–470, <https://doi.org/10.1680/geot.1985.35.4.461>
- Taylor, R.N. 1987. Discussion on Tan & Scott (1985). *Géotechnique*, **37**, 131–133, <https://doi.org/10.1680/geot.1987.37.1.131>
- Van Genuchten, M.T. 1980. A closed-form equation for predicting the hydraulic conductivity of unsaturated soils. *Soil Science Society of America Journal*, **44**, 892–898, <https://doi.org/10.2136/sssaj1980.03615995004400050002x>
- Villar, L.F. 2002. *Study of the Densification and Desiccation of Residual Mineral Waste from the Processing of Bauxite*. PhD thesis, PUC-Rio, Rio de Janeiro.
- Wellings, S.R. 1984. Recharge of the Upper Chalk aquifer at a site in Hampshire, England. *Journal of Hydrology*, **69**, 275–285, [https://doi.org/10.1016/0022-1694\(84\)90167-7](https://doi.org/10.1016/0022-1694(84)90167-7)
- White, D. 2020. Geotechnical centrifuge modelling – current practice. In: Addis, B. (ed.) *Physical Models: Their Historical and Current Use in Civil and Building Engineering Design*. Ernst, Berlin, 965–984.
- Zornberg, J.G. and McCartney, J.S. 2010. Centrifuge permeameter for unsaturated soils. I: theoretical basis and experimental developments. *Journal of Geotechnical and Geoenvironmental Engineering*, **136**, 1051–1063, [https://doi.org/10.1061/\(ASCE\)GT.1943-5606.0000319](https://doi.org/10.1061/(ASCE)GT.1943-5606.0000319)